Systems/Circuits

Contralateral Limb Specificity for Movement Preparation in the Parietal Reach Region

Eric Mooshagian,[1,2*] Eric A. Yttri,[1,3*] Arthur D. Loewy,[1] and Lawrence H. Snyder[1]

[1]Department of Neuroscience, Washington University School of Medicine, St. Louis, Missouri 63110, [2]Department of Cognitive Science, University of California San Diego, La Jolla, California 92093, and [3]Department of Biological Sciences, Carnegie Mellon University, Pittsburgh, Pennsylvania 15213

The canonical view of motor control is that distal musculature is controlled primarily by the contralateral cerebral hemisphere; unilateral brain lesions typically affect contralateral but not ipsilateral musculature. Contralateral-only limb deficits following a unilateral lesion suggest but do not prove that control is strictly contralateral: the loss of a contribution of the lesioned hemisphere to the control of the ipsilesional limb could be masked by the intact contralateral drive from the nonlesioned hemisphere. To distinguish between these possibilities, we serially inactivated the parietal reach region, comprising the posterior portion of medial intraparietal area, the anterior portion of V6a, and portions of the lateral occipital parietal area, in each hemisphere of 2 monkeys (23 experimental sessions, 46 injections total) to evaluate parietal reach region's contribution to the contralateral reaching deficits observed following lateralized brain lesions. Following unilateral inactivation, reach reaction times with the contralesional limb were slowed compared with matched blocks of control behavioral data; there was no effect of unilateral inactivation on the reaction time of either ipsilesional limb reaches or saccadic eye movements. Following bilateral inactivation, reaching was slowed in both limbs, with an effect size in each no different from that produced by unilateral inactivation. These findings indicate contralateral organization of reach preparation in posterior parietal cortex.

Key words: **intraparietal sulcus; muscimol; posterior parietal cortex; reach; visuomotor**

Significance Statement

Unilateral brain lesions typically affect contralateral but not ipsilateral musculature. Contralateral-only limb deficits following a unilateral lesion suggest but do not prove that control is strictly contralateral: the loss of a contribution of the lesioned hemisphere to the control of the ipsilesional limb could be masked by the intact contralateral drive from the nonlesioned hemisphere. Unilateral lesions cannot distinguish between contralateral and bilateral control, but bilateral lesions can. Here we show similar movement initiation deficits after combined unilateral and bilateral inactivation of the parietal reach region, indicating contralateral organization of reach preparation.

Introduction

The canonical view of motor control is that distal musculature is controlled primarily by the contralateral cerebral hemispheres (Fig. 1). Supporting this view is the fact that unilateral lesions frequently affect only body movements contralateral to the side of the lesion (Daroff et al., 2012). Increasing evidence suggests, however, that there may be latent control of the ipsilateral side as well, in both frontal (Matsunami and Hamada, 1981; Tanji et al., 1988; Donchin et al., 1998) and parietal areas (Chang et al., 2008). In humans, fMRI studies similarly show clear bilateral activity, albeit with a contralateral bias (Astafiev et al., 2003; Connolly et al., 2003; Medendorp et al., 2005; Prado et al., 2005; Fernandez-Ruiz et al., 2007; Filimon et al., 2009; Gallivan et al., 2009, 2011; Bernier and Grafton, 2010; Cavina-Pratesi et al., 2010; Cappadocia et al., 2016). Likewise, transcranial magnetic stimulation studies do not yield strict contralateral limb specificity (Busan et al., 2009; Vesia et al., 2010; Buetefisch et al., 2014). Arm movement kinematics can be decoded from ipsilateral motor cortex (Ganguly et al., 2009; Bundy et al., 2018). We aimed to reconcile bilateral reach representations with contralateral but not ipsilateral deficits after unilateral lesions.

Received Jan. 28, 2021; revised Oct. 30, 2021; accepted Dec. 5, 2021.

Author contributions: E.M., A.D.L., and L.H.S. analyzed data; E.M., E.A.Y., and L.H.S. wrote the first draft of the paper; E.M. and L.H.S. edited the paper; E.M. and L.H.S. wrote the paper; E.A.Y. and L.H.S. designed research; E.A.Y. performed research.

This work was supported by National Institutes of Health Grant EY012135. All the relevant code is available upon reasonable request to the senior author. We thank Jonathon Tucker for assistance with MRI acquisition and figure construction.

*E.M. and E.A.Y. contributed equally to this work.

The authors declare no competing financial interests.

Correspondence should be addressed to Eric Mooshagian at emooshagian@ucsd.edu.

https://doi.org/10.1523/JNEUROSCI.0232-21.2021

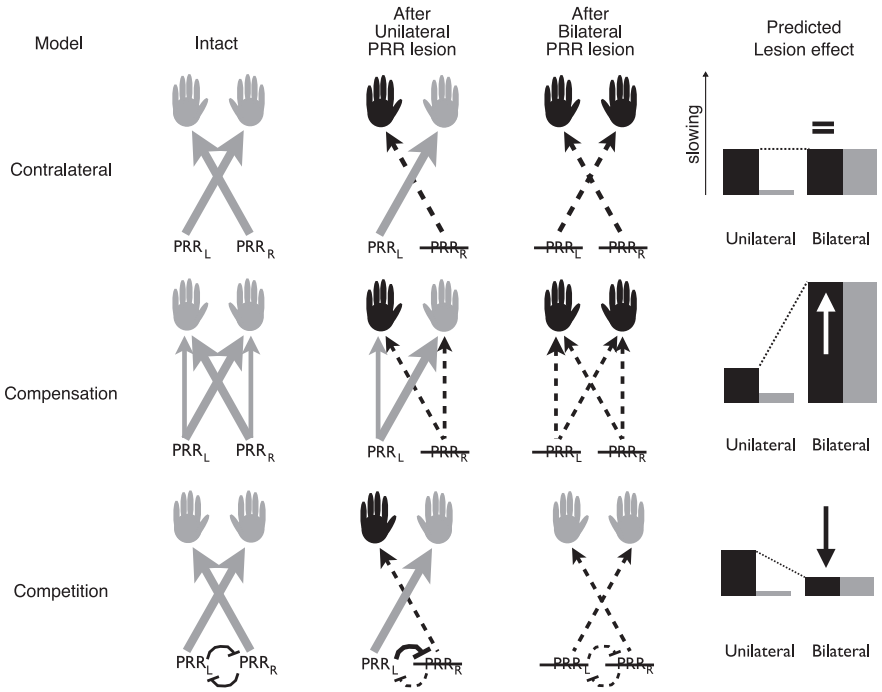

Figure 1. Three architectures underlying contralateral deficits after unilateral brain lesions. Schematics for contralateral-specific (top row), hemispheric compensation (middle row), and interhemispheric competition (bottom row) models are shown following a unilateral lesion (in this case, right PRR). The first three columns represent the visuomotor pathway in their intact, unilaterally, and bilaterally lesioned states, respectively. Solid lines indicate intact pathways by which PRR affects reaching. Dashed lines indicate compromised pathways. Line width indicates the relative strength of these connections. Gray hands represent normal reach performance. Black hands represent abnormal (slowed) reaches. Bar plots represent the predicted degree of impairment for each limb (black: contralateral to first lesion; gray: ipsilateral to first lesion) after unilateral (left) and bilateral (right) lesions.

There are at least three architectures that could lead to purely contralateral deficits after a unilateral lesion. Each hemisphere may exert strict lateralized limb control ("contralateral" model). Alternatively, control could be bilateral, but the ipsilateral contribution could be redundant ("compensation" model). In this model, the loss of drive from the lesioned hemisphere that helps control the contralateral limb may be partially compensated by the intact secondary drive from the opposite hemisphere (Faugier-Grimaud et al., 1978; Bartolomeo and Schotten, 2016). Alternatively, each hemisphere could have a strict contralateral organization but also inhibit the opposite hemisphere ("competition" model). This mutual inhibition could be unbalanced by a small lesion in one hemisphere, resulting in complete suppression of the damaged hemisphere and a deficit specific to the contralesional limb (Sprague, 1966; Hilgetag et al., 2001). A unilateral lesion does not distinguish among strict lateralized limb control, bilateral control with compensation, and cross-hemisphere inhibitory interactions.

Each of these models makes a unique prediction about the effect of a bilateral versus unilateral lesion. The strictly contralateral model predicts that lesioning the second (opposite) hemisphere will not affect the original deficit (Fig. 1, top: lesion effects are shown as increases in reaction time (RT) compared with a baseline, right column). By contrast, the compensation model predicts that a second lesion will exacerbate the original deficit, since it removes both the dominant contralateral drive plus the covert ipsilateral drive (Fig. 1, middle). Finally, the competition model predicts that the second lesion will restore hemispheric balance and thereby ameliorate the effect of the first lesion (Fig. 1, bottom) (Sprague, 1966; Hilgetag et al., 2001).

We used these predictions to probe the laterality of motor planning, an essential part of motor control. The parietal reach region (PRR) is a functionally defined portion of the posterior parietal cortex (PPC) in the macaque monkey comprising the caudal portion of the medial intraparietal area (MIP) and extending caudally into dorsal V6a, whose neurons are active when reaches are planned and executed (Snyder et al., 1997; Bakola et al., 2017). At the population level, PRR is half as active before a reach with the ipsilateral arm as it is before a reach with the contralateral arm (Chang et al., 2008; Mooshagian et al., 2018). Critically, a unilateral lesion affects only reaches with the contralateral arm (Lamotte and Acuña, 1978; Brown et al., 1983; Yttri et al., 2014).

In the current study, PRR was lesioned first in one hemisphere and then in the other, with behavioral testing before and after each lesion. Surprisingly, the second lesion had no additional effect on the limb contralateral to the first lesion. These results strongly support the contralateral model and indicate that PRR's contribution to motor planning is strictly contralateral.

Materials and Methods

Experimental model and subject details

Two adult, male macaque monkeys (Monkey G, Macaca mulatta; and Monkey Q, Macaca fascicularis) were tested. All procedures were in accordance with the *Guide for the care and use of laboratory animals* and were approved by the Washington University Institutional Animal Care and Use Committee.

Behavioral tasks

Animals sat in complete darkness with their heads restrained in custom-made primate chairs (Crist Instruments). The fronts of the chairs could open from waist to neck so that the forelimbs had complete freedom of movement. Visual stimuli were back-projected onto a translucent Plexiglas screen mounted vertically ~17 cm in front of the animal. Eye movements were monitored with a scleral search coil (CNC Engineering). Hand position was recorded every 2 ms with 3.5 mm resolution using an optical touch screen.

Monkeys performed memory-guided center-out reaching and saccade tasks (Fig. 2*a*). Reaches were made with either the left or right limb in alternating blocks. The unused limb was blocked by a Plexiglas panel. For all tasks, trials started with the animal fixating and touching a central fixation cue (5.5° window for the eye, 6° for the hand). After a 350 ms fixation period, a peripheral target flashed for 150 ms at 1 of 8 equally spaced locations 20° from the fixation point. The target position instructed the location. The target color instructed the type of movement to make: red instructed a saccade; green instructed a reach; half green, half red instructed a coordinated reach. After a subsequent 1000-1600 ms delay, the fixation target was extinguished, cueing the animal to move. On "saccade only" trials, the animal had 500 ms to make a saccade to within 10° of the remembered target location; 150 ms after the eyes acquired the peripheral window, the target reappeared and a corrective saccade to within 5° was required. Each animal performed different variants of the reach task. Monkey Q performed a "coordinated reach" task, wherein the animal made a combined reach plus saccade, with the arm arriving within 10° of the target no later than 250 ms after the saccade; 150 ms after the initial landing of the hand in the peripheral window, the

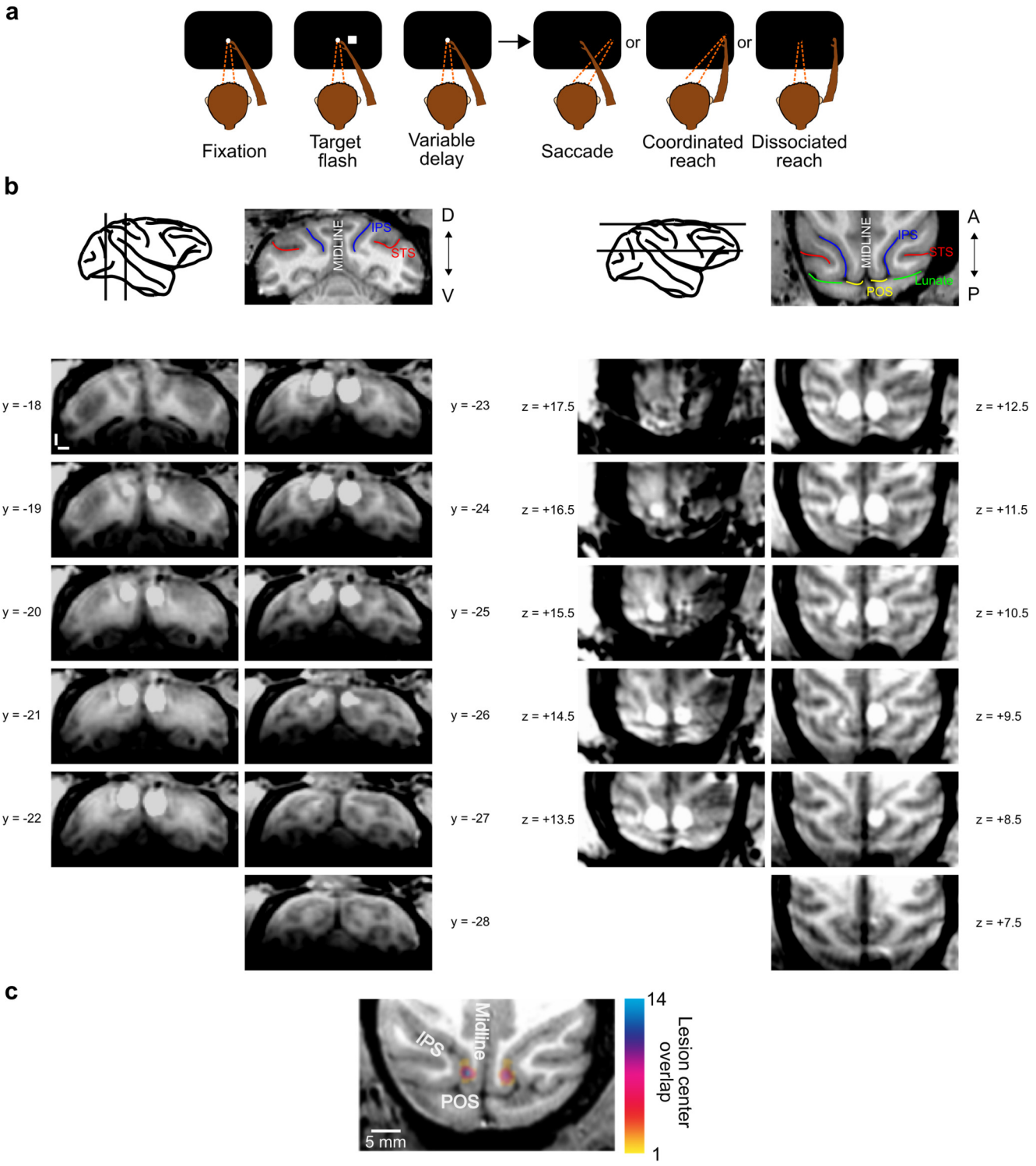

Figure 2. Task design. ***a***, Memory-guided saccade and coordinated saccade-reach tasks. After an initial fixation and reach period, a target appeared briefly at 1 of 8 peripheral locations arranged in a circle around the initial fixation and reach point. The target location instructed the movement goal, and the color instructed movement type: green represents reach; red represents saccade (color not shown in figure); half green, half red represents a coordinated reach. After a variable delay period, the central fixation point disappeared, cueing the animal to make the instructed movement to the remembered target. Saccade-alone trials were randomly interleaved with either dissociated (Monkey G) or coordinated (Monkey Q) reach trials. ***b***, Injection localization. Top, Schematics indicating approximate slice positions and sulcul anatomy for a representative PRR injection in Monkey Q. IPS, Intraparietal sulcus; LOP, lateral occipital-parietal area; Midline, longitudinal fissure; POS, parieto-occipital sulcus; STS, superior temporal sulcus. Bottom, Slice reconstruction of an example injection. MRI sections through the coronal plane (left), and axial plane (right) shows the injections as bright white halos on the medial bank of the IPS in both hemispheres. *Y* and *Z* values indicate the slice distance in millimeters caudal to the AC (coronal slices) and dorsal to the AC-PC plane (axial slices). Scale bar, 5 mm. ***c***, A complete reconstruction of individual injection sites from Monkey Q aligned and superimposed on a representative horizontal MR image plane. Each injection site is represented by a 1-mm-diameter circle, and all sites are summed. Colors represent greater overall overlap of individual halos, ranging from 1 (yellow) to 14 (blue). Scale bar, 5 mm.

target reappeared and a corrective saccade to within 6.0° and a corrective reach to within 6.5° was required. Monkey G performed a "dissociated reach" task wherein the animal reached while maintaining fixation at the central cue. These trials were performed in the same manner as coordinated reaches, but the animal maintained visual fixation. If the animal failed to perform a trial, the trial was aborted, reward was withheld, and a 1 s timeout ensued. Data collection was completed within 2.5 h of the first inactivation, well within the period of maximum efficacy for muscimol (Arikan et al., 2002).

Reversible inactivation. PRR was initially localized by using single-unit recordings. We identified PRR as that region of cortex containing a high proportion of visually responsive cells with delay-period activity that was greater for reach-only or reach-plus-saccade trials than for saccade-only trials. This region includes the posterior portion of MIP, the anterior portion of V6a, and portions of the lateral occipital parietal area. Injections sites were chosen to minimize spread beyond PRR's boundaries. Injection spread was established by coinjecting manganese with the muscimol and imaging the animals shortly after the conclusion of the experiment (Liu et al., 2010). Injections were aimed at the posterior portion of the medial bank of the intraparietal sulcus near the MIP/V6a border. The diameters of the injection volumes reached ~5-6 mm in diameter (see Injection localization with MRI) (Fig. 2*b*,*c*). To minimize tissue damage, sites were varied by 1-2 mm across sessions. The precise location of this border varies across studies in the literature so that definitive assignments of individual recording sites to one anatomic area or another are difficult to make (Lewis and Essen, 2000; Tanné-Gariépy et al., 2002; Bakola et al., 2017).

Each inactivation proceeded as follows: an injection cannula was slowly lowered to the desired position and allowed to settle for 10 min. Next, 0.5-2.0 µl of 8 mg/ml muscimol plus 0.1 M of the MRI contrast agent manganese (9.8 mg/ml $MnCl_2(H_2O)_4$) was injected through a 33 G cannula (Small Parts) attached to a 25 µl Hamilton syringe driven by a microinjection pump (Harvard Apparatus) at a rate of 0.05-0.15 µl/min (10-15 min). To minimize the occurrence of upward flow of injectate with cannula retraction, the cannula was left in place for 10 min after the completion of the injection and then slowly retracted. Next, the behavioral test block commenced (~30 min). After the behavioral task block, the process (inactivation and behavioral block) was repeated for the PRR of the opposite hemisphere. Monkey G participated in 7 sessions, and Monkey Q participated in 16 sessions. The order of left and right hemisphere lesions changed across experimental sessions. Right PRR was inactivated first in 14 sessions (Monkey Q = 9, Monkey G = 5), and left PRR was inactivated first in 10 sessions (Monkey Q = 7, Monkey G = 3).

Inactivation and control sessions differed only by whether a muscimol-manganese or sham injection was performed. For control sessions, the injection drive was mounted to the monkeys' head and the microinjection pump was turned on, but the cannula was not lowered into the brain. Saline injections were not used for two reasons. First, the nonlesioned hemisphere serves as the control after unilateral inactivation. Second, since we were not specifically interested in the pharmacologic effects of muscimol, any perturbations of PRR activity, including, for example, volume effects, would constitute a legitimate test of our hypothesis (though our small, slow injections were unlikely to generate such effects). Control sessions were identical to inactivation sessions in number of trials, time of day, duration, and tasks performed. Control sessions never occurred the day following inactivation to avoid possible aftereffects of the previous inactivation.

Injection localization with MRI. T1-weighted anatomic images were collected within 2-4 h of each injection using an MPRAGE sequence (FOV, 160 × 160 mm^2; matrix size, 320 × 320; slice time echo, 3.94 ms; TR, 1.89 s; inversion time, 1 s; flip angle, 7°; 80 slices; 0.50 × 0.50 × 0.50 mm voxels) conducted on a 3T head-only system (Siemens Allegra). A single surface coil was used. Animals were lightly sedated with ketamine (3 mg/kg) during the procedure. Injections were visible as a bright halo representing the Mn-induced T1 signal increase (Fig. 2*b*).

Permanent lesion. Permanent lesions more closely mimic the effects of naturally occurring lesions and ensure a more complete lesion. They cannot be repeated within the same animal and almost certainly are accompanied by long-term adaptation. Temporary lesions can be repeated in the same animal multiple times, and their transient nature minimizes long-term adaptive changes in the brain (Chowdhury and DeAngelis, 2008). Thus, both types of lesions have experimental advantages. After completing the reversible inactivation experiments, we performed permanent lesions in one animal (Monkey G) with ibotenic acid, an excitotoxin. Like muscimol, ibotenic acid spares fibers of passage, ensuring that the lesion effects reflect the loss of PRR neurons and not fibers of passage. We permanently lesioned left and right PRR in separate sessions separated by 1 week. In each session, a 15 mg/ml solution of ibotenic acid plus manganese (19.8 mg/ml $MnCl_2(H_2O)_4$) was injected through a 32 G Hamilton needle attached to a 10 µl Hamilton syringe. The injection procedure was the same as that for muscimol inactivation. Behavioral data were collected following each permanent lesion. Data from the day of the lesion were excluded from analysis.

Data processing

Saccade movement onset and offset were defined by velocity criteria. Reach movement onset and offset were defined by the change in touch position. Movement accuracy was quantified as the Euclidian distance in degrees of visual angle between the mean movement endpoint and the target location. Errors could be temporal (movement before or after the allotted period, or failure to maintain fixation at the location of the peripheral target for at least 150 ms) or spatial (movements landing >10° away from the remembered peripheral target location, or failure to make a corrective movement to the peripheral target location after it reappeared at the end of the trial). Errors that occurred before the initial target appearance were excluded.

Behavioral data from each inactivation session were compared with the data from the two previous control sessions. The significance of inactivation effects across sessions was computed using a paired two-tailed Student's *t* test. A one-way ANOVA was used to assess whether movement initiation depended on target direction (0°, 45°, 90°, 135°, 180°, 225°, 270°, 315° relative to the positive *x* axis). A repeated-measures ANOVA with the factors target direction and injection (first, second) was used to study the effect of target direction after each inactivation. A *t* test was conducted to assess whether movement initiation depended on hemifield (contralesional vs ipsilesional). Targets presented along the vertical meridian (90°, 270°) were excluded for this analysis. The α level for all tests was $p < 0.05$, and all tests were two-sided, unless otherwise noted. RT values are reported as the mean RT during inactivation minus the mean RT during control sessions. Positive values reflect slowing, and negative values reflect speeding, of RT during inactivation compared with control conditions. Values were computed similarly for saccade RT. Endpoint accuracy was expressed as the Euclidian distance between the target and the mean endpoint. Endpoint precision was expressed as the SD of the Euclidian distance of each endpoint from the mean endpoint.

No statistical methods were used to predetermine the sample size, but the numbers of monkeys used for these experiments are comparable to those used in the field and in previous studies. Data collection and analysis were not performed in a manner blind to the conditions of the experiments. Both animals performed all tasks and were not randomly assigned to a specific experiment group.

Results

We serially inactivated PRR in each hemisphere of 2 monkeys (23 experimental sessions, 46 injections total; 7 sessions for Monkey G and 16 for Monkey Q) to evaluate PRR's contribution to the contralateral reaching deficits observed following lateralized brain lesions (Fig. 2*b*). Following each inactivation, monkeys performed center-out memory-guided saccades and reaches (Yttri et al., 2013) (Fig. 2*a*). When reaching, one animal moved its eyes along with its arm ("coordinated reach"), while the other animal maintained central fixation ("dissociated reach").

Following unilateral inactivation, reach initiations with the contralesional limb were slowed compared with matched blocks of control behavioral data (both: 7.2 ms, $t_{(22)} = 3.12$, $p = 0.01$; G: 10.8 ms, $t_{(6)} = 1.86$, $p = 0.11$; Q: 5.6 ms, $t_{(15)} = 2.59$,

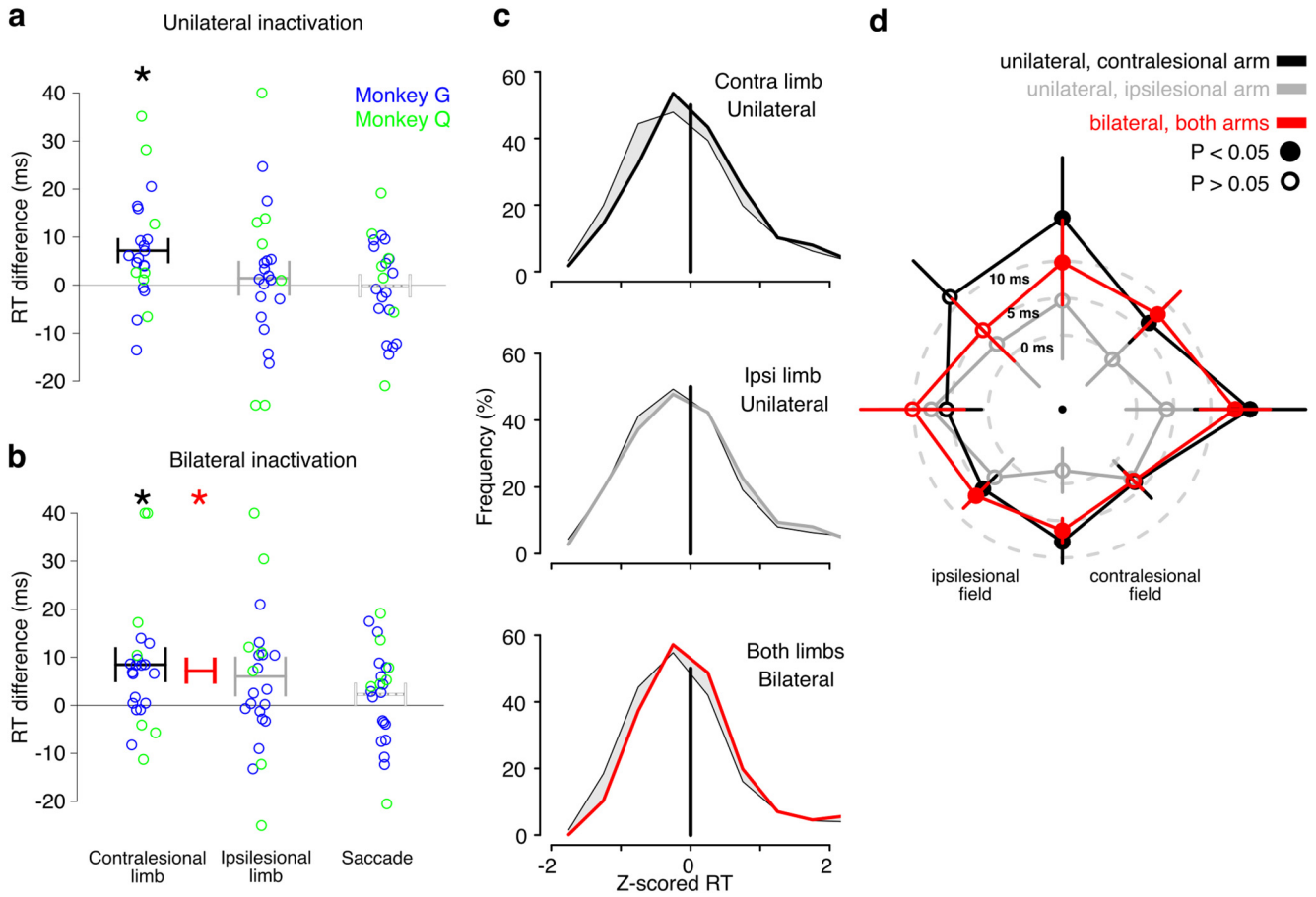

Figure 3. PRR lesion effects on response time are contralesional. ***a***, Change in RT following unilateral inactivation versus control. Blue and green circles represent the individual session values for Monkeys G and Q, respectively. Symbols for values >40 ms or <−25 ms are displayed at 40 or −25 ms, respectively, for display purposes only. Horizontal lines indicate condition means. Vertical lines indicate SEM. ***b***, Same as in ***a*** following bilateral inactivation. Red symbols represent the two arms combined. For bilateral inactivation, "contralesional limb" refers to the limb contralateral to the first injection, and "ipsilesional limb" refers to the limb ipsilateral to the first and contralateral to the second injection. ***c***, Shift in the distribution of RTs following unilateral inactivation for the contralateral (top) and ipsilateral limb (middle) and following bilateral inactivation for both limbs (bottom). RT values increase from left to right. Thin (control) and heavy (inactivation) lines indicate the distribution of RTs, *z*-scored to the control data (vertical black line indicates the median RT). In the contralateral and bilateral cases, the heavy traces fall to the right of the light traces. Effects are small but consistent across the range of RTs. ***d***, Polar plot of the change in RT for reaches with the contralateral (black) or ipsilateral limb (gray) to each of 8 equally spaced locations 20° from the fixation point following unilateral and both limbs averaged (red) after bilateral inactivation. Contralesional targets are displayed on the right, and ipsilesional targets are displayed on the left. The innermost dashed circle (0 ms) represents no effect. Filled data points represent significance ($p < 0.05$, *t* test, uncorrected).

$p = 0.02$, paired *t* test; Fig. 3*a*). There was no effect of unilateral inactivation on the RT of either ipsilesional-limb reaches (both: 1.4 ms, $t_{(22)} = 0.67$, $p = 0.44$; G: 5.0 ms, $t_{(6)} = 0.29$, $p = 0.78$; Q: 0.8 ms, $t_{(15)} = 0.32$, $p = 0.75$) or saccadic eye movements (both: 0.1 ms, $t_{(22)} = 0.04$, $p = 0.95$; G: 3.1 ms, $t_{(6)} = 0.69$, $p = 0.53$; Q: −1.2 ms, $t_{(15)} = -0.53$, $p = 0.63$). Effects were similar for lesions on the right or left (e.g., slowing of the contralesional limb by 6.0 vs 4.7 ms for 8 and 14 sessions, respectively; *p* of the difference = 0.46). These findings are consistent with previous studies (cited above).

In contrast to many other inactivation studies, we next placed a second lesion in the homotopic area of the opposite hemisphere and then collected additional behavioral data. After a lesion is placed in each hemisphere, both limbs are contralateral to a reversible lesion. We therefore report the result for bilateral lesion analyses for each arm separately, as well as combined. The terms "ipsilesional limb" and "contralesional limb" refer to the limb with respect to the side of the first injection. Following bilateral inactivation, reaching was slowed when data from the limbs are combined (both: 7.2 ms, $t_{(45)} = 2.91$, $p = 0.01$; Fig. 3*b*). Both dissociated (G: 14.3 ms, $t_{(13)} = 1.92$, $p = 0.08$) and coordinated reaches were slowed (Q: 4.1 ms, $t_{(31)} = 3.16$, $p < 0.01$), and in each case the slowing was no different from that produced by unilateral inactivation ($p = 0.60$ and $p = 0.57$, respectively). In none of our three scenarios did we predict a difference in effects in the two arms (Fig. 1). We found comparable slowing in each (8.5 vs 6.0 ms, respectively, for the arm contralateral to the first and the second injection; not significantly different [$t_{(44)} = 0.49$, $p = 0.63$]), although the effects reached significance in only one arm ($t_{(22)} = 2.57$, $p = 0.02$ vs $t_{(22)} = 1.59$, $p = 0.13$, respectively). There was no effect of bilateral inactivation on the RT of saccades (both: 2.4 ms, $t_{(22)} = 1.12$, $p = 0.28$; G: 5.7 ms $t_{(6)} = 1.2$, $p = 0.28$; Q: 0.9 ms, $t_{(15)} = 0.41$, $p = 0.69$).

Figure 3*c* shows normalized RT distributions for inactivation (heavy traces) versus control trials (thin traces). RT values increase from left to right. In all cases, the RTs are slowed following inactivation. The RT slowing was evenly distributed across all reaches, rather than being restricted to one tail of the distribution (Fig. 3*c*). This pattern of effects suggests that PRR

inactivation affects only the contralesional limb (Fig. 1, top row), and argues against the compensation and competition models (Fig. 1, middle and bottom rows).

The effect size, as quantified by Cohen's *d*, that is, normalized to the SD of the difference, was 0.21 after unilateral inactivation (contralesional limb) and 0.20 after bilateral inactivation. These effect sizes are small but nontrivial, and they are 2-4 times as large as those for the ipsilesional limb after unilateral injection (0.08) or for saccades after unilateral or bilateral injection (0.05 and 0.06, respectively).

Slowing was significantly greater for the contralesional compared with the ipsilesional limb in 10 of 23 experiments and significantly greater for the ipsilesional limb compared with the contralesional limb in 2 ($p < 0.05$, *t* test). After the second injection, both arms were significantly slowed in 10 of 23 experiments, with 2 showing speeding ($p < 0.05$, *t* test).

Lesion effects did not depend on the spatial location of the target of the movement. A repeated-measures ANOVA on Animal (G, Q) × Injection (first, second) × Arm (contralesional, ipsilesional) × Direction (0°, 45°, 90°, 135°, 180°, 225°, 270°, 315°) showed a main effect of Arm [$F_{(1,19)} = 5.37$, $p = 0.03$], but no other main effects or interactions. Figure 3*d* depicts the mean effect of inactivation on RT for reaches to each of the eight target locations for each limb. Reach initiation with the contralesional limb was slowed, independent of target location ($F_{(7,147)} = 0.99$, $p = 0.4$, one-way ANOVA; $p < 0.05$ for six of eight directions, one-tailed *t* test). Reach initiation with the ipsilesional limb, by contrast, was neither slowed down nor sped up for any target location ($F_{(7,147)} = 0.40$, $p = 0.90$, one-way ANOVA; $p > 0.25$ for each individual location, *t* test without multiple-comparisons correction). After bilateral inactivation, reach initiation was slowed ($F_{(7,147)} = 0.59$, $p = 0.77$, one-way ANOVA; $p < 0.05$ for five of eight locations, *t* test without multiple-comparisons correction). More power can be obtained by averaging over targets in the contralateral versus ipsilateral hemifields, yet in no case did reach initiation depend on the hemifield of the target (Table 1). These results justify the pooling of data across animals and target directions.

Reach accuracy was not significantly affected by these injections (Fig. 4*a*,*b*). There was no significant effect on speed after either the first or second injection. There was a tendency toward hypometria and an overall upward shift, neither of which was significant. Effects on endpoint dispersion (the inverse of precision) approached significance for reaches with the contralesional but not ipsilesional limb ($p = 0.11$ and $p = 0.31$, respectively) after unilateral inactivation. There was a small but significant increase in endpoint dispersion after bilateral inactivation ($p = 0.02$) (Fig. 4*c*).

After unilateral inactivation, there was an ensemble effect of target direction on saccadic eye movements in the pure saccade task ($F_{(7,147)} = 2.5$, $p = 0.02$, one-way ANOVA), but this was not significant for any single direction compared with control (all $p > 0.15$, paired *t* test). The ensemble effect was unchanged by bilateral inactivation [repeated-measures ANOVA, target direction: $F_{(7,147)} = 5.34$, $p = 0.02$; injection × target direction ($F_{(7,147)} = 0.48$, $p = 0.85$)]. There was no effect of inactivation on coordinated saccades, that is, saccades accompanying the reach (repeated-measures ANOVA, all $p > 0.1$).

Effects of permanent lesions

After completing the temporary inactivation experiments, we conducted permanent lesions in Monkey G to match the effects of naturally occurring lesions more closely. Results corroborated those from the temporary inactivations (Fig. 5). The unilateral lesion significantly increased contralesional limb RT (5.2 ms, $p = 0.003$). There was no effect on saccades (−1.2 ms, $p = 0.32$; data not shown) or ipsilateral reach RT (2.4 ms, $p = 0.2$). After the bilateral permanent lesion, the slowing of the two limbs (5.1 ms, $p = 0.002$) was not significantly different from the unilateral lesion effect on the contralesional limb ($p = 0.98$), consistent with a strict contralesional contribution from PRR. We confirmed the lesion sites postmortem (Fig. 5*b*). Lesions were largely restricted to the medial bank of the intraparietal sulcus, extending posteriorly into V6a, with only minimal spread across the sulcus into caudal intraparietal sulcus.

Table 1. Mean RT changes versus control by visual hemifield[a]

Lesion	Arm	Contralesional field	Ipsilesional field	*p* value of difference
Both animals				
Unilateral	Contralesional arm	8.99*	7.10*	0.67
Unilateral	Ipsilesional arm	3.25	5.47**	0.54
Bilateral	Contralesional arm	9.69*	10.93**	0.77
Bilateral	Ipsilesional arm	8.19*	5.06	0.56
Bilateral	Both arms	8.94*	7.92**	0.77
Monkey G				
Unilateral	Contralesional arm	19.84*	13.01	0.57
Unilateral	Ipsilesional arm	3.65	9.23	0.55
Bilateral	Contralesional arm	21.09**	20.85	0.98
Bilateral	Ipsilesional arm	12.68	13.90	0.94
Bilateral	Both arms	16.89**	17.37	0.97
Monkey Q				
Unilateral	Contralesional arm	3.93	4.34	0.92
Unilateral	Ipsilesional arm	3.07	3.72	0.85
Bilateral	Contralesional arm	4.37	6.30*	0.61
Bilateral	Ipsilesional arm	6.10*	0.94	0.13
Bilateral	Both arms	5.23*	3.51**	0.34

[a]RT values are shown in milliseconds. For bilateral inactivation, "contralesional limb" refers to the limb contralateral to the first injection, and "ipsilesional limb" refers to the limb ipsilateral to the first and contralateral to the second injection.
*$p < 0.05$ (one-tailed *t* test).
**$p < 0.10$ (one-tailed, *t* test).

Discussion

Our sequential bilateral lesion results indicate that PRR contributes primarily to the planning of movements with the contralateral limb. This provides new insight into motor planning in the PPC. The cortical control of contralateral limb movements is a main organizing principle of primate motor systems. Yet there is substantial evidence that control is not exclusively contralateral, particularly in frontal cortex. There are neurons in supplementary motor area, premotor cortex, and M1 that are active during ipsilateral limb movements (Matsunami and Hamada, 1981; Tanji et al., 1988; Donchin et al., 1998), and arm movement kinematics can be decoded from ipsilateral motor cortex (Ganguly et al., 2009; Bundy et al., 2018). In the PPC, most studies test only movements of the arm that is contralateral to the side of recording. Single-unit recording studies that have tested both arms indicate a strong contralateral bias (Kermadi et al., 2000; Chang et al., 2008; Mooshagian et al., 2018).

The current study provides strong evidence that ipsilateral limb movements are represented in PRR, but that PRR does not contribute to ipsilateral limb planning. This finding was presaged by the findings that unilateral inactivation only affects the contralateral arm (Yttri et al., 2013, 2014), and that PRR activity predicts reach RT, but only for the contralateral limb (Snyder et al.,

2006; Chang et al., 2008). A similar distinction between the laterality of representation and causal control has been reported in other cortical areas (MacAvoy et al., 1991; Gottlieb et al., 1994).

A possible alternative explanation for intact ipsilateral function after unilateral inactivation is compensatory effects from homotopic tissue in the opposite hemisphere (Wilke et al., 2012). In this account, paired lesions in both hemispheres should produce more severe deficits (e.g., greater RT slowing) compared with a unilateral lesion (Fig. 1). Alternatively, the interhemispheric competition hypothesis posits tonic inhibition between left and right cortex that is disrupted by unilateral lesions (Kinsbourne, 1977). In this account, a second lesion to the opposite hemisphere should restore interhemispheric balance and thereby ameliorate the effects of unilateral inactivation. We find that rather than exacerbating or ameliorating the effect of a unilateral lesion, a second lesion in the opposite hemisphere has no additional effect on the arm contralateral to the first lesion, consistent with the interpretation that PRR causally effects only the contralateral limb.

In our hands, inactivation affects mainly changes in RT. This contrasts with other studies finding no change in RT (Hwang et al., 2012; Christopoulos et al., 2015). We also find a tendency toward hypometria, but this was not significant and did not depend on whether reaches were coordinated or dissociated. Little or no effect on amplitude or accuracy is consistent with previous observations from these same animals using similarly sized unilateral injections (Yttri et al., 2014) but contrasts with reports of hypometria for reaches in all directions after larger injections (Hwang et al., 2012) or after removal of a large swath of cortex (Brodmann's areas 5 and 7) (Lamotte and Acuña, 1978). The differences between this and previous studies may be partly attributable to task design. Previous studies inactivated only one hemisphere and examined only contralateral arm performance (Hwang et al., 2012) or both contralateral and ipsilateral arm performance (Yttri et al., 2014), and in one instance, inactivated both hemispheres, but on separate days, and without repetition (Battaglia-Mayer et al., 2013). Here, we made within-subject, within-session comparisons to evaluate the differential effects of unilateral and bilateral inactivation on limb specificity. Each inactivation served as its own control. We might have expected bilateral inactivation to result in equal slowing of the ipsilesional and contralesional limbs. Ipsilesional limb slowing after bilateral inactivation did not reach significance; however, the contralesional and ipsilesional limb effects after bilateral inactivation were not different from one another.

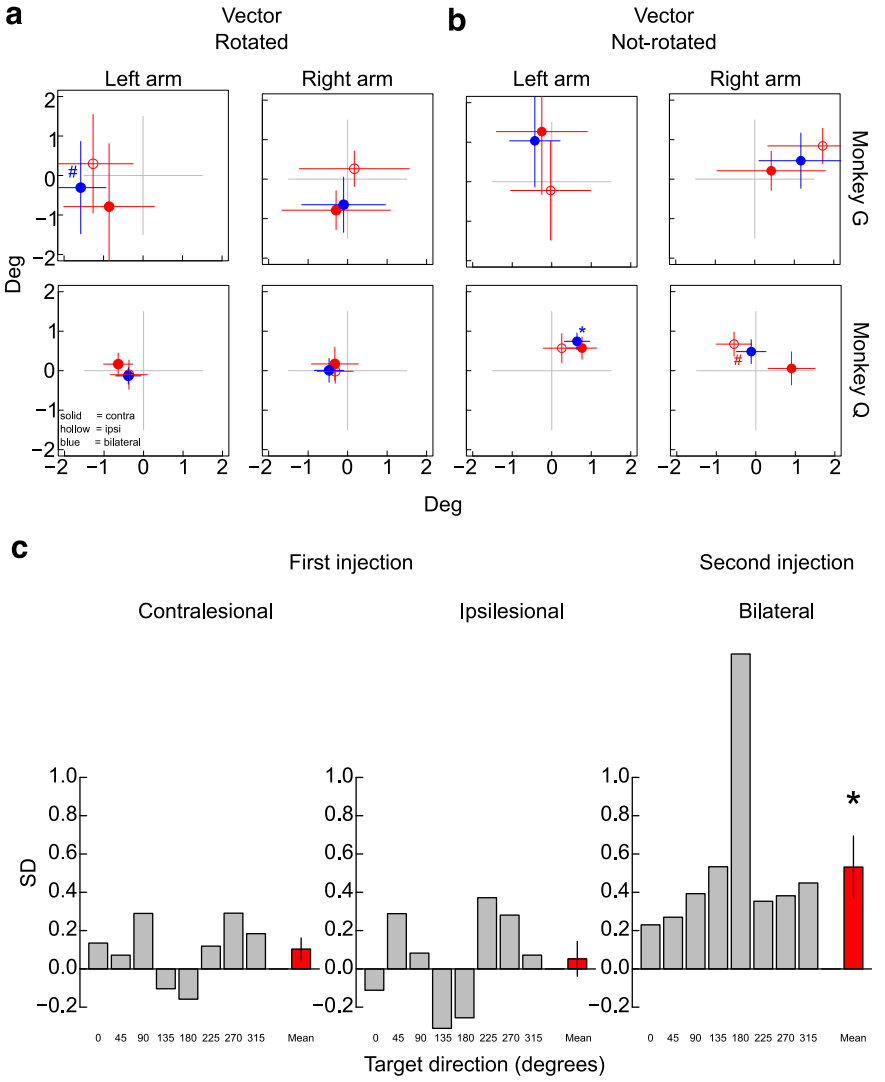

Figure 4. Reach accuracy and precision. ***a***, ***b***, Reach accuracy, that is, the average constant error computed across individual reaches and sessions, for each monkey (rows), and for each arm (columns). ***a***, Data are rotated so that targets are all aligned before averaging to test for consistent hypometria/hypermetria. Errors to the left represent hypometric reaches. ***b***, Same data as in ***a***, but reach endpoints are averaged without rotation to test for overall biases in each direction. When split by arm (left and right; columns), by location relative to the lesion (ipsilesional [hollow red], contralesional [filled red], or both [blue]), and by monkey (rows), by target laterality (right or left visual hemifield; data not shown), only one condition showed a significant horizonal effect of the injection with a $p < 0.01$ (not corrected for multiple comparisons; correction would eliminate the significance), and there were no consistent trends. Two significant vertical effects are shown, both in Monkey Q; the significant horizontal effect occurred when the data were split by hemifield, doubling the number of comparisons. The SEs of the endpoints were large, particularly for the animal performing dissociated reaches, so it is possible that small but significant effects might emerge with more data. ***c***, Reach dispersion, quantified as the SD of reach endpoints from the mean. Contralesional arm after the first injection (left), ipsilesional arm after the first injection (middle), and both arms after bilateral injection (right). Gray bars represent the SD of reach endpoints (variable error) for each of the 8 movement directions (experimental – control) in degrees. Red bars represent the mean effect across all movement directions. Target position is counterclockwise from the positive *x* axis (e.g., 45 degrees is up and to the right). $^{\#}p < 0.05$. $^{*}p < 0.01$.

The 2 animals in our study performed different reaching tasks. Monkey G performed a dissociated reach task requiring central visual fixation during the reach, while Monkey Q was required to pair a saccade with each reach. It is conceivable that the two tasks might have been differentially affected by PRR inactivation. However, the differences observed between the tasks/monkeys were few and unsystematic. Most results were

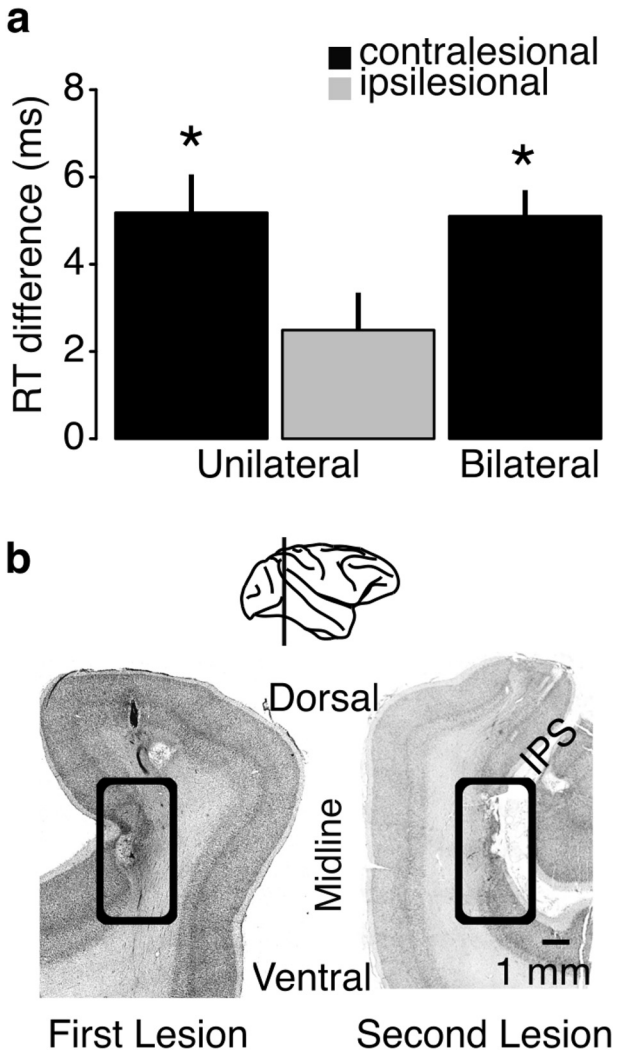

Figure 5. Permanent lesion effects. ***a***, Mean change in RT for reaches with the contralateral (black, left) and ipsilateral limbs (gray, middle) after a unilateral permanent lesion, and after bilateral permanent lesions (black, right). Asterisks indicate significant slowing compared with control sessions. ***b***, Coronal section through PRR showing the location of each ibotenic acid lesion, shown within the black boxes. Extent of damaged tissue on the left is limited to about halfway down the medial wall of the IPS, although some gliosis because of the electrode tracks is visible above the lesion. The lesion on the right involves the mirror symmetric location. In each case, the lesion extends through most layers of the cortex. With the second lesion, there was some damage to the gyrus of the superior parietal lobule. Inset, approximate slice position.

qualitatively, if not quantitatively, similar. For instance, response times were slowed in both animals, but the effect was only significant in Monkey G. The magnitude of slowing was approximately twice as large in Monkey Q. Future studies should assess these task differences across multiple animals.

Our conclusions contrast with some findings from stroke patients in whom a compensatory role of the contralesional hemisphere is supported (Murase et al., 2004; Johansen-Berg, 2007; Umarova et al., 2011). The discrepancy could reflect species differences, the fact that clinical lesions are typically heterogenous and span multiple cortical regions as well as white matter, or the fact that we test immediately after the lesion, whereas patients are often tested months or even years after the insult (Corbetta et al., 2005; Balan et al., 2019). Our findings also contrast with functional imaging studies in monkeys that suggest rapid reorganization of the intact hemisphere after unilateral inactivation of the lateral intraparietal area (LIP) (Balan and Gottlieb, 2009; Wilke et al., 2012). This may not be surprising, however. Eye movement control in the cortex is organized in a fundamentally different way from arm movement control. Most cortical oculomotor areas, including LIP, influence both eyes equally but drive movements only in the contralateral direction. In contrast, many cortical somatomotor areas are biased to control body parts on the opposite side of the body and can drive those body parts in any direction. Given this large difference in organization, it is not unreasonable that rapid reorganization in response to lesions might also be different in LIP versus PRR.

There are some important limitations of the current study. The magnitude of the RT slowing (5-10 ms) is modest. Behavior can become automated and stereotyped with overtraining, which may explain why lesions produce only a slight impairment. Furthermore, brain plasticity or changes in connectivity may occur with extensive practice (Chowdhury and DeAngelis, 2008; Wilke et al., 2012). Of course, it is difficult to perform these experiments in animals that have not been extensively trained. We used small injection volumes (0.5-2 µl) to minimize spread into neighboring areas. In comparison, other studies have used volumes up to fivefold larger and obtained larger effect sizes than what we report, including prominent hypometria, though these studies tested only the contralateral limb (e.g., Hwang et al., 2012). Larger injections may produce larger effects, particularly regarding contralateral limb hypometria, where we saw only a nonsignificant trend. It also remains to be seen if, and how, reorganization occurs in the long-term after cortical lesions. Reach-related activity in the PPC is found in neurons throughout an extended network of parietal areas (Battaglia-Mayer and Caminiti, 2009). We only tested one cortical region implicated in reach planning, and our results may not generalize to other reach-related areas. The organization may be different, for example, in frontal motor areas, where individual neurons are known to encode bimanual reach and participate in online control of reaching (Donchin et al., 1998).

PRR is functionally defined and includes neurons that exhibit clear visual responses to visual targets and sustained delay activity before reaching movements (Snyder et al., 1997). Inclusion in PRR is not limited to neurons from a particular anatomically defined area, and instead comprises neurons crossing anatomic boundaries (see Materials and Methods). Other authors have defined PRR differently, for example, as lying further anterior on the medial bank in area 5 (e.g., Hwang et al., 2012). The precise human homolog of PRR is not known, but functional imaging studies have identified reach planning activity in superior parieto-occipital cortex (putative V6a homolog) using functional imaging (Astafiev et al., 2003; Connolly et al., 2003; Medendorp et al., 2005; Cappadocia et al., 2016). TMS over PPC revealed hand preference in medial intraparietal sulcus, but not in the more posteriorly located superior parieto-occipital cortex (Vesia and Crawford, 2012). Injection locations were concentrated in a restricted area of MIP. We did not vary injection location over the extent of MIP to investigate any gradient of effects along MIP. It therefore remains to be seen whether our results hold across all PPC reach-related regions.

Distal hand musculature is believed to be under almost exclusive contralateral cortical control, especially compared with proximal and axial muscles (Brinkman and Kuypers, 1973). Our task design used a center-out arm movement that engaged proximal and axial musculature as well as distal muscles. It is possible that still more proximal movements might show bilateral control. More generally, we cannot be certain that a different task might not yield different results. For example, control might

differ with bilateral movements. Indeed, one study found impaired visual control of hand movements after bilateral, but not unilateral, PRR inactivation (Battaglia-Mayer et al., 2013). Nevertheless, our results clearly indicate that, for at least some reaching tasks, PRR controls only the contralateral limb, although ipsilateral arm movements can be decoded from PRR activity.

References

Arikan R, Blake NM, Erinjeri JP, Woolsey TA, Giraud L, Highstein SM (2002) A method to measure the effective spread of focally injected muscimol into the central nervous system with electrophysiology and light microscopy. J Neurosci Methods 118:51–57.

Astafiev SV, Shulman GL, Stanley CM, Snyder AZ, Essen DC, Corbetta M (2003) Functional organization of human intraparietal and frontal cortex for attending, looking, and pointing. J Neurosci 23:4689–4699.

Bakola S, Passarelli L, Huynh T, Impieri D, Worthy KH, Fattori P, Galletti C, Burman KJ, Rosa MGP (2017) Cortical afferents and myeloarchitecture distinguish the medial intraparietal area (MIP) from neighboring subdivisions of the macaque cortex. Eneuro 4:ENEURO.0344-17.2017.

Balan PF, Gottlieb J (2009) Functional significance of nonspatial information in monkey lateral intraparietal area. J Neurosci 29:8166–8176.

Balan PF, Gerits A, Zhu Q, Kolster H, Orban GA, Wardak C, Vanduffel W (2019) Fast compensatory functional network changes caused by reversible inactivation of monkey parietal cortex. Cereb Cortex 29:2588–2606.

Bartolomeo P, Schotten M (2016) Let thy left brain know what thy right brain doeth: inter-hemispheric compensation of functional deficits after brain damage. Neuropsychologia 93:407–412.

Battaglia-Mayer A, Caminiti R (2009) Posterior parietal cortex and arm movement. In: Encyclopedia of Neuroscience (Squire LR, ed) pp 783–795. Academic Press.

Battaglia-Mayer A, Ferrari-Toniolo S, Visco-Comandini F, Archambault PS, Saberi-Moghadam S, Caminiti R (2013) Impairment of online control of hand and eye movements in a monkey model of optic ataxia. Cereb Cortex 23:2644–2656.

Bernier PM, Grafton ST (2010) Human posterior parietal cortex flexibly determines reference frames for reaching based on sensory context. Neuron 68:776–788.

Brinkman J, Kuypers HG (1973) Cerebral control of contralateral and ipsilateral arm, hand and finger movements in the split-brain rhesus monkey. Brain 96:653–674.

Brown JV, Ettlinger G, Garcha HS (1983) Visually guided reaching and tactile discrimination performance in the monkey: the effects of removals of parietal cortex soon after birth. Brain Res 267:67–79.

Buetefisch CM, Revill KP, Shuster L, Hines B, Parsons M (2014) Motor demand-dependent activation of ipsilateral motor cortex. J Neurophysiol 112:999–1009.

Bundy DT, Szrama N, Pahwa M, Leuthardt EC (2018) Unilateral, 3D arm movement kinematics are encoded in ipsilateral human cortex. J Neurosci 38:10042–10056.

Busan P, Jarmolowska J, Semenic M, Monti F, Pelamatti G, Pizzolato G, Battaglini PP (2009) Involvement of ipsilateral parieto-occipital cortex in the planning of reaching movements: evidence by TMS. Neurosci Lett 460:112–116.

Cappadocia DC, Monaco S, Chen Y, Blohm G, Crawford JD (2016) Temporal evolution of target representation, movement direction planning, and reach execution in occipital–parietal–frontal cortex: an fMRI study. Cereb Cortex 27:5242–5260.

Cavina-Pratesi C, Monaco S, Fattori P, Galletti C, McAdam TD, Quinlan DJ, Goodale MA, Culham JC (2010) Functional magnetic resonance imaging reveals the neural substrates of arm transport and grip formation in reach-to-grasp actions in humans. J Neurosci 30:10306–10323.

Chang SW, Dickinson AR, Snyder LH (2008) Limb-specific representation for reaching in the posterior parietal cortex. J Neurosci 28:6128–6140.

Chowdhury SA, DeAngelis GC (2008) Fine discrimination training alters the causal contribution of macaque area MT to depth perception. Neuron 60:367–377.

Christopoulos VN, Bonaiuto J, Kagan I, Andersen RA (2015) Inactivation of parietal reach region affects reaching but not saccade choices in internally guided decisions. J Neurosci 35:11719–11728.

Connolly JD, Andersen RA, Goodale MA (2003) fMRI evidence for a 'parietal reach region' in the human brain. Exp Brain Res 153:140–145.

Corbetta M, Kincade MJ, Lewis C, Snyder AZ, Sapir A (2005) Neural basis and recovery of spatial attention deficits in spatial neglect. Nat Neurosci 8:1603–1610.

Daroff RB, Fenichel GM, Jankovic J, Mazziotta JC (2012) Neurology in clinical practice. Amsterdam: Elsevier.

Donchin O, Gribova A, Steinberg O, Bergman H, Vaadia E (1998) Primary motor cortex is involved in bimanual coordination. Nature 395:274–278.

Faugier-Grimaud S, Frenois C, Stein DG (1978) Effects of posterior parietal lesions on visually guided behavior in monkeys. Neuropsychologia 16:151–168.

Fernandez-Ruiz J, Goltz HC, DeSouza JF, Vilis T, Crawford JD (2007) Human parietal 'reach region' primarily encodes intrinsic visual direction, not extrinsic movement direction, in a visual motor dissociation task. Cereb Cortex 17:2283–2292.

Filimon F, Nelson JD, Huang RS, Sereno MI (2009) Multiple parietal reach regions in humans: cortical representations for visual and proprioceptive feedback during on-line reaching. J Neurosci 29:2961–2971.

Gallivan JP, Cavina-Pratesi C, Culham JC (2009) Is that within reach? fMRI reveals that the human superior parieto-occipital cortex encodes objects reachable by the hand. J Neurosci 29:4381–4391.

Gallivan JP, McLean DA, Smith FW, Culham JC (2011) Decoding effector-dependent and effector-independent movement intentions from human parieto-frontal brain activity. J Neurosci 31:17149–17168.

Ganguly K, Secundo L, Ranade G, Orsborn A, Chang EF, Dimitrov DF, Wallis JD, Barbaro NM, Knight RT, Carmena JM (2009) Cortical representation of ipsilateral arm movements in monkey and man. J Neurosci 29:12948–12956.

Gottlieb JP, MacAvoy MG, Bruce CJ (1994) Neural responses related to smooth-pursuit eye movements and their correspondence with electrically elicited smooth eye movements in the primate frontal eye field. J Neurophysiol 72:1634–1653.

Hilgetag CC, Théoret H, Pascual-Leone A (2001) Enhanced visual spatial attention ipsilateral to rTMS-induced 'virtual lesions' of human parietal cortex. Nat Neurosci 4:953–957.

Hwang EJ, Hauschild M, Wilke M, Andersen RA (2012) Inactivation of the parietal reach region causes optic ataxia, impairing reaches but not saccades. Neuron 76:1021–1029.

Johansen-Berg H (2007) Functional imaging of stroke recovery: what have we learnt and where do we go from here? Int J Stroke 2:7–16.

Kermadi I, Liu Y, Rouiller EM (2000) Do bimanual motor actions involve the dorsal premotor (PMd), cingulate (CMA) and posterior parietal (PPC) cortices? Comparison with primary and supplementary motor cortical areas. Somatosens Mot Res 17:255–271.

Kinsbourne M (1977) Hemi-neglect and hemisphere rivalry. Adv Neurol 18:41–49.

Lamotte RH, Acuña C (1978) Defects in accuracy of reaching after removal of posterior parietal cortex in monkeys. Brain Res 139:309–326.

Lewis JW, Essen DC (2000) Mapping of architectonic subdivisions in the macaque monkey, with emphasis on parieto-occipital cortex. J Comp Neurol 428:79–111.

Liu Y, Yttri EA, Snyder LH (2010) Intention and attention: different functional roles for LIPd and LIPv. Nat Neurosci 13:495–500.

MacAvoy MG, Gottlieb JP, Bruce CJ (1991) Smooth-pursuit eye movement representation in the primate frontal eye field. Cereb Cortex 1:95–102.

Matsunami K, Hamada I (1981) Characteristics of the ipsilateral movement-related neuron in the motor cortex of the monkey. Brain Res 204:29–42.

Medendorp WP, Goltz HC, Crawford JD, Vilis T (2005) Integration of target and effector information in human posterior parietal cortex for the planning of action. J Neurophysiol 93:954–962.

Mooshagian E, Wang C, Holmes CD, Snyder LH (2018) Single units in the posterior parietal cortex encode patterns of bimanual coordination. Cereb Cortex 28:1549–1567.

Murase N, Duque J, Mazzocchio R, Cohen LG (2004) Influence of interhemispheric interactions on motor function in chronic stroke. Ann Neurol 55:400–409.

Prado J, Clavagnier S, Otzenberger H, Scheiber C, Kennedy H, Perenin MT (2005) Two cortical systems for reaching in central and peripheral vision. Neuron 48:849–858.

Snyder LH, Batista AP, Andersen RA (1997) Coding of intention in the posterior parietal cortex. Nature 386:167–170.

Snyder LH, Dickinson AR, Calton JL (2006) Preparatory delay activity in the monkey parietal reach region predicts reach reaction times. J Neurosci 26:10091–10099.

Sprague JM (1966) Interaction of cortex and superior colliculus in mediation of visually guided behavior in the cat. Science 153:1544–1547.

Tanji J, Okano K, Sato KC (1988) Neuronal activity in cortical motor areas related to ipsilateral, contralateral, and bilateral digit movements of the monkey. J Neurophysiol 60:325–343.

Tanné-Gariépy J, Rouiller EM, Boussaoud D (2002) Parietal inputs to dorsal versus ventral premotor areas in the macaque monkey: evidence for largely segregated visuomotor pathways. Exp Brain Res 145:91–103.

Umarova RM, Saur D, Kaller CP, Vry MS, Glauche V, Mader I, Hennig J, Weiller C (2011) Acute visual neglect and extinction: distinct functional state of the visuospatial attention system. Brain 134:3310–3325.

Vesia M, Crawford JD (2012) Specialization of reach function in human posterior parietal cortex. Exp Brain Res 221:1–18.

Vesia M, Prime SL, Yan X, Sergio LE, Crawford JD (2010) Specificity of human parietal saccade and reach regions during transcranial magnetic stimulation. J Neurosci 30:13053–13065.

Wilke M, Kagan I, Andersen RA (2012) Functional imaging reveals rapid reorganization of cortical activity after parietal inactivation in monkeys. Proc Natl Acad Sci USA 109:8274–8279.

Yttri EA, Liu Y, Snyder LH (2013) Lesions of cortical area LIP affect reach onset only when the reach is accompanied by a saccade, revealing an active eye-hand coordination circuit. Proc Natl Acad Sci USA 110:2371–2376.

Yttri EA, Wang C, Liu Y, Snyder LH (2014) The parietal reach region is limb specific and not involved in eye-hand coordination. J Neurophysiol 111:520–532.